Check for updates

Received: 21 January 2019 | Revised: 24 March 2019 | Accepted: 12 April 2019
DOI: 10.1002/jemt.23281

RESEARCH ARTICLE

MICROSCOPY RESEARCH & TECHNIQUE WILEY

Deep learning model integrating features and novel classifiers fusion for brain tumor segmentation

Sajid Iqbal[1,2] | Muhammad U. Ghani Khan[2] | Tanzila Saba[3] | Zahid Mehmood[4] | Nadeem Javaid[5] | Amjad Rehman[6] | Rashid Abbasi[7]

[1]Department of Computer Science, Bahauddin Zakariya University, Multan, Pakistan
[2]Department of Computer Science and Engineering, University of Engineering and Technology, Lahore, Pakistan
[3]College of Computer and Information Sciences, Prince Sultan University, Riyadh, Saudi Arabia
[4]Department of Computer Engineering, University of Engineering and Technology, Taxila, Pakistan
[5]Department of Computer Science, COMSATS University, Islamabad, Pakistan
[6]College of Computer and Information Systems, Al Yamamah University, Riyadh, Saudi Arabia
[7]School of Computer and Technology, Anhui University, Hefei, China

Correspondence
Sajid Iqbal, Department of Computer Science, Bahauddin Zakariya University, Multan, Pakistan.
Email: sajidiqbal@bzu.edu.pk

Review Editor: Peter Saggau

Abstract

Automatic and precise segmentation and classification of tumor area in medical images is still a challenging task in medical research. Most of the conventional neural network based models usefully connected or convolutional neural networks to perform segmentation and classification. In this research, we present deep learning models using long short term memory (LSTM) and convolutional neural networks (ConvNet) for accurate brain tumor delineation from benchmark medical images. The two different models, that is, ConvNet and LSTM networks are trained using the same data set and combined to form an ensemble to improve the results. We used publicly available MICCAI BRATS 2015 brain cancer data set consisting of MRI images of four modalities T1, T2, T1c, and FLAIR. To enhance the quality of input images, multiple combinations of preprocessing methods such as noise removal, histogram equalization, and edge enhancement are formulated and best performer combination is applied. To cope with the class imbalance problem, class weighting is used in proposed models. The trained models are tested on validation data set taken from the same image set and results obtained from each model are reported. The individual score (accuracy) of ConvNet is found 75% whereas for LSTM based network produced 80% and ensemble fusion produced 82.29% accuracy.

KEYWORDS
brain tumor segmentation, convolutional neural networks, ensemble neural networks, LSTM

1 | INTRODUCTION

Uncontrolled growth of tissue cells results in a tumor that may be benign or malignant/cancerous. Brain cancer is among the different causes for an increase in mortality rate in the world. The death rate, due to a brain tumor, has been increased to 300% in the last few decades (Saba et al., 2019; Saba, Bokhari, Sharif, Yasmin, & Raza, 2018c; Tahir et al., 2019). According to National Cancer Institute America (NCIA) and American Cancer Society (ACS), around 1.5 million cancer cases are identified in 2013 and more than 1.6 million cancer patients are registered in 2014 in America. The count is increased from 1.6 to 1.65 in 2015. By looking at statistics of 2014, 33% (0.6 million) of diagnosed patients have lost their lives (Khan, Akram, et al., 2019b; Khan, Lali, et al., 2019c).

A benign tumor is a mass that does not spread and does not cause any harm whereas a malignant tumor is harmful and is also known as cancer. A malignant tumor is categorized into different classes based on various characteristics like type of originating tissue, location, and level of severity. Brain tumors are also categorized based on their origin: primary brain tumors are the lesions that emerge within the brain whereas secondary brain tumors (metastatic tumors) originate at a different location of the body and move to the brain. There are different categorization schemes designed by researchers but the scheme designed by the World Health Organization (WHO) is considered to

 © 2019 Wiley Periodicals, Inc.

be the standard (Aurangzeb, Muhammad Attique, Saba, Javed, & Iqbal, 2019; Fahad, Khan, Saba, Rehman, & Iqbal, 2018; Husham, Alkawaz, Saba, Rehman, & Alghamdi, 2016; Jamal, Hazim Alkawaz, Rehman, & Saba, 2017; Khan et al., 2018, 2019a; Rehman, Abbas, Saba, Rahman, et al., 2018c; Rehman, Abbas, Saba, Mehmood, et al., 2018b; Rehman, Abbas, Saba, Mahmood, & Kolivand, 2018a; Saba, 2017; Saba, Al-Zahrani, & Rehman, 2012; Saba, Rehman, Mehmood, Kolivand, Uddin, et al., 2018a; Saba, Rehman, Mehmood, Kolivand, & Sharif, 2018b). WHO has made more than 120 categories for a brain tumor and each category is further graded from I to IV (Louis et al., 2016).

Tumors that are allotted grade I and II (low grade) are safe and nonenhancing whereas those given grade III and IV are known as malignant and enhancing (Abbas et al., 2019; Yousaf et al., 2019). The development of a cancerous tumor is gradual. First, a benign tumor originates to the malignant stage with the passage of time. With the rise of tumor grade, its treatment is relatively impossible. Therefore, it is intensively required to develop methods and procedures to detect such lesions in the brain at an early stage for proper cure.

Medical treatment of brain tumor requires the proper diagnosis of tumor type and its grade (Iqbal, Ghani, Saba, & Rehman, 2018; Iqbal, Khan, Saba, & Rehman, 2017; Khan et al., 2019a). Among all treatment methods, medical imaging is considered safe and taken as the first priority to visualize internal structure of the brain to come up with the diagnostic conclusion (Abbas et al., 2015; Mughal, Muhammad, Sharif, Saba, & Rehman, 2017a; Mughal, Sharif, Muhammad, & Saba, 2017b; Rahim, Norouzi, Rehman, & Saba, 2017a; Rahim, Rehman, Kurniawan, & Saba, 2017b). Among various medical imaging methods, MRI has evolved as a popular noninvasive technique for brain imaging. It provides high-resolution spatial images and produces high contrast values for soft tissues (Norouzi et al., 2014). There are different sequences and modalities of MRI in practice and each modality provides information from one particular perspective. Hence, experts use images taken through different modalities collectively to retrieve information from different perspectives. These sequences may include T1-MRI, T1c-MRI, T2 MRI, and FLAIR MRI. For example, to localize the anatomical structures scans with best resolution, that is, T1 are used. To locate the lesion region within the brain, pathological T2 scan is preferred. The MRI multimodal images are processed to create the more human-friendly and accurate 3D view of the brain by merging the 2D images using morphological operations.

To extract the required information from medical images like MRI, researchers have deployed various statistical learning methods that could be categorized as conventional machine learning methods and state of the art deep learning or ANN based methods. Conventional machine learning methods can show good results for segmentation and classification tasks however they suffer from two fundamental limitations (a) they are specific to the used data set and (b) are not easily scalable. The modern state of the art methods addresses these limitations to a greater extent. ANN-based algorithms could be easily scaled and produce better results than traditional machine learning methods. However, they also become data specific to some extent. Recently we find a lot of interest in the application of ANNs for medical image segmentation and classification related tasks. Different architectures of ANN are being explored that include fully connected networks, convolutional neural networks, auto-encoders, LSTM based networks and their variants (Li et al., 2016; Nasir et al., 2018; Khan et al., 2019a).

Usually, a picture contains objects which consist of clusters of pixels that are highly co-related. A group of pixels forming an object (i.e., line, corner) has similar color densities or follows a pattern of color change (Ebrahim, Kolivand, Rehman, Rahim, & Saba, 2018; Haji, Alkawaz, Rehman, & Saba, 2019; Katuka, Mohamad, Saba, El-Affendi, & Mohamed, 2014; Saba, 2016; Younus et al., 2015). For complex objects, for example, if a chair is present in a picture, all pixels belonging to the chair will form a single cluster or set of clusters with some common features. It means that co-related pixels have a high tendency to occur in cluster form. In other words, there is a higher probability that class of a pixel can be determined from the class of neighboring pixel, that is, $\text{class}(p_i) = w * \text{class}(p_{i-1})$. Here, parameter w defines the weight of co-relation or similarity. Long short term memory (LSTM) networks have been successfully applied for natural language processing and co-related sequences of data. The phenomenon of pixel co-relation motivated us to explore the long short term memory networks for image segmentation (Jamal et al., 2017). In the proposed research, two-type of small networks: convolutional and LSTM based ANNs to perform image segmentation and pixel classification task. The results thus obtained from the two networks show the usability of LSTM networks that have higher performance than conventional networks. In order to boost performance, we devise an ensemble of both networks. Both networks learn the image parameters in different manners which make us inquisitive about using both models together and find how the ensemble of these models can impact the results as compared to their individual applications. To measure the performance of these methods, we used open source benchmark data set, that is, BRATS2015 provided by MICCAI. The results comparison shows 2–3% improvement in the accuracy of segmentation by combining the models over individual model performance. Major contributions of this research are listed below:

- Proposal of sequence learning model as patch wise image segmentation model.
- A brief comparison of the performance of CNN, sequence learning and ensemble model.
- Deployment and comparison of different class imbalance handling techniques.

The rest of the paper is organized as such: Section 2 presents the literature review, in Section 3 proposed methodology is described in detail. Section 4 describes the implementation details and discusses the results. Finally, the conclusion is given in Section 5.

2 | LITERATURE SURVEY

Researchers are using two main ANN based methods to segment and classify medical images (Husham et al., 2016; Jamal et al., 2017; Norouzi et al., 2014; Rahim, Norouzi, et al., 2017a; Rahim, Rehman, et al., 2017b;

Saba, 2017; Sadad, Munir, Saba, & Hussain, 2018). First one is called the patch-based method. In this method, patches of small sizes, that is, 5×5 are extracted from the input image and are classified. The second method is known as semantic segmentation where complete image is fed to the network and each image pixel is classified individually (Fahad et al., 2018; Waheed, Alkawaz, Rehman, Almazyad, & Saba, 2016). To conclude, first method is coarse classification whereas the second method produces fine-grained classification. Results obtained through the second method are better than produced with first method.

To test the performance of the designed model, different brain tumor data sets have been used by researchers (Abbas et al., 2018a; Abbas et al., 2018b; Saba et al., 2019). Data sets published by Medical Image Computing and Computer-Assisted Intervention (MICCAI) conference under Brain Tumour Segmentation (BRATS) Challenge have become the benchmark to test the model performance and make a comparison with other models. Each year, the conference publishes a new data set which is named accordingly like BRATS2015 and BRATS2016 referring to data sets published in the year 2015 and 2016. These data sets define four classes of tumors divided into three categories, that is, whole tumor, core tumor and enhancing tumor. The BRATS platform provided by BRATS challenge uses few measures to evaluate the model performance. These measures include dice score, Hausdorff distance, sensitivity and specificity. Among these measures, the dice score is the most important and useful. In the following section, we review the ANN brain tumor segmentation methods that have used BRATS data sets and are evaluated on the BRATS platform. Different researchers have done performance evaluation in different ways. Some are evaluating their model on the platform provided by BRATS challenge whereas others devising the validation data set from the training set (Chaudhry, Rahim, Saba, & Rehman et al., 2018; Sharif et al., 2018; Yousuf et al., 2018).

A variety of ANN architectures are being explored by the researchers to find the best results (Al-Ameen et al., 2015; Iftikhar, Fatima, Rehman, Almazyad, & Saba, 2017; Jamal et al., 2017; Mughal, Muhammad, et al., 2017a; Mughal, Muhammad, Sharif, Rehman, & Saba, 2018; Mughal, Sharif, et al., 2017b; Muhsin, Rehman, Altameem, Saba, & Uddin, 2014; Rad, Rahim, Rehman, Altameem, & Saba, 2013; Waheed et al., 2016). Such models include encoder–decoder models (Castillo et al., 2017; Saba, 2018; Saba, Rehman, & Sulong, 2011a; Sharif et al., 2017), multiple networks to extract the different level of features (Sedlar, 2017), models using convolutional networks with some postprocessing (Shaikh et al., 2017) and hybrid architectures with varying numbers of layers (Mundher, Muhamad, Rehman, Saba, & Kausar, 2014; Neamah, Mohamad, Saba, & Rehman, 2014; Saba & Alqahtani, 2013). Not All these models are comparable in term of layers, however; end results are important to make a distinction among them. Other performance evaluation parameters may include the number of layers, trained model size and prediction time of the network (Khan, Akram, et al., 2019b; Khan, Lali, et al., 2019c).

A complex heavy network consisting of 28 layers is proposed in Castillo et al. (2017). It uses patches of MRI images to segment the tumor area. The model runs three copies of CNN architecture to extract features of different levels that are combined at varying levels to form final output. This work uses a subset of training set images to train their model. The method is strong as it uses BRATS provided test set to measure the model performance. Sajid et al. (2018) used encoder–decoder based architecture to segment the brain images. They proposed the modified UNET based architecture to perform the task. The model is a comparatively lightweight network which incorporates sequence and excitation block to extract high-quality image features. The residual encoder and convolutional decoder have been used to segment BRATS2017 multimodal images in Pawar et al. (2017). They proposed a deep residual model for feature extraction to segment the input image. The network is heavy and compute-intensive due to 49-layer architecture. Network prediction time is also higher. Sedlar (2017) used two CNN networks in parallel to extract local and global features of input data. They used validation data set to evaluate the performance of their method <evaluation and number of layers>. Another CNN based model is proposed by Shaikh et al. (2017) called "Convolutional neural network with fully dense layers". They used fully convolutional neural network (FCNN) followed by dense conditional random field (DCRF) as post-processing step for segmentation. Postprocessing step helps in fine-tuning the predictions. Real strength of this method lies in network architecture. Multiscale hierarchical features also play a significant role in classifying the image pixels. A symmetry driven CNN model is used by down sampling and three-time up sampling path for segmentation purpose (Schubert et al., 2009). A design of three different CNN architectures to segment the 3D-MRI image is presented in Shen, Zhang, and Zheng (2017). In this work, instead of directly using the 3D-image as input, they converted it into a stack of 2D images by slicing each 3D image. Patches from each image slice are extracted and fed as network input. The same network is trained with different size of patches of, that is, 28*28, 12*12, and 5*5 pixels, respectively. The results show the best performance of the CNN model with 28*28 patch size. They use custom validation set taken from training images to measure the performance. Pereira, Pinto, Alves, and Silva (2016a) presented a patch based model. They preprocessed the images by using histogram equalization and normalization. CNN model is given input of 33×33 axial patches to learn features. To avoid overfitting, the dropout layer is introduced as a regularization method in addition to a few morphological operations (Joudaki et al., 2014; Meethongjan, Dzulkifli, Rehman, Altameem, & Saba, 2013; Saba, Rehman, & Sulong, 2011a).

A few works are reported that use LSTM based layers for image segmentation and related tasks. Byeon and Breuel (2014) used 2D LSTM network to segment images into different regions based on texture information present in image data set. Stollenga et al. (2015) employed

TABLE 1 Sample of combination of preprocessing techniques

S#	Noise removal	Contrast enhancement	Edge enhancement
1	GF	HE	LP
2	ANS	HE	USM
3	WF	MHE	LP

Note. GF = Gaussian filter; HE = histogram equalization; LP = Laplacian edge enhancement; ANS = anisotropic diffusion; USM = unsharp masking; WF=Weiner filter; MHE = multiple histogram equalization.

multidimensional recurrent neural networks (MD-RNNs) to manipulate the underlying spatiotemporal context for pixel-wise classification of brain images. Chen et al. (2016) proposed a deep learning framework for 3D image segmentation that is based on the combination of fully convolutional network and recurrent neural network. FCN is used to exploit intra-slice context whereas RCNN is used for inter-slice context. However, we observe that LSTM networks can exploit all 3D contexts equally. The task of semantic labeling (classification) is performed by Li et al. (2016) using a modified version of the LSTM based neural network. They used long short term memorized context fusion to capture and fuse contextual information from multichannel image data and show a good level of improvement in their task. In the same year, Liang, Shen, Feng, Lin, and Yan (2016) has used modified LSTM architecture called Graph Long Short Term Memory (Graph LSTM) for semantic object scene parsing. In this work, they formed the super-pixels leading to the construction of the undirected graph for each image. Another application of LSTM based networks could be seen in Ren and Zemel (2017) for instance segmentation. Despite all these improvements, brain tumor segmentation is still a challenging task.

3 | PROPOSED METHODOLOGY

The proposed methodology is composed of four main stages described as follows:

1. Data set description
2. Preprocessing
3. Classification models
4. Testing and evaluation

3.1 | Data set description

The data set used in this study is obtained from MICCAI BRATS2015 challenge. This multimodal data set consists of 274 cases for training and 110 cases for the test. The training images contain high grade and low-grade glioma with ground truth. Each case is imaged using T1, T2, T1c, and FLAIR sequences. Size of each image sequence is $155 \times 240 \times 240$ with manually annotated ground truth of the same size. The ground truth is annotated with five labels (Menze et al., 2015) as follows:

- 1 for necrosis
- 2 for edema
- 3 for nonenhancing tumor
- 4 for enhancing tumor
- 0 for everything else.

In the conducted experiments, BRATS2015 training data set is divided into training, validation and test sets in the ratio of 60, 20, and 20 respectively. Each 3D image is first converted into 2D slices and before feeding to network, small patches of size 25×25 are extracted from 2D images to form the input batch of tensors having shape $(20 \times 4 \times 25 \times 25)$ with ground truth batch of similar tensor shape $(20 \times 1 \times 25 \times 25)$ to do patch-wise semantic segmentation. To avoid storage and memory limitations of computing device, patches from each image are extracted in place and fed to the networks.

3.2 | Preprocessing

To remove unwanted information present in acquired images, different preprocessing methods are used (Saba, Almazyad, & Rehman, 2016;

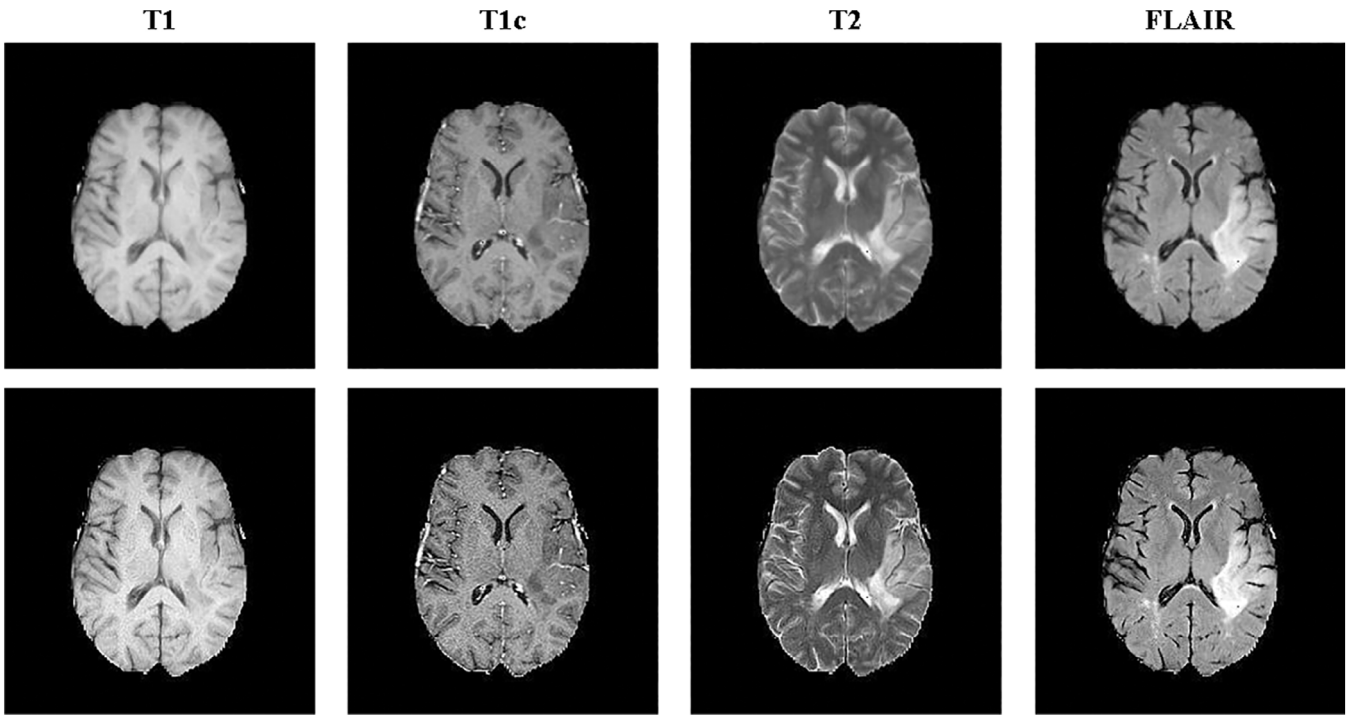

FIGURE 1 (a) Top row: original slice images. (b) Bottom row: slice images after preprocessing

TABLE 2 CNN and LSTM augmented network architecture

Layer	Parameters	Layer	Parameters
Input layer	Input: (none, 25, 25, 4)	Input layer	Input: (none, 25, 25, 4)
	Output: (none, 25,25,4)		Output: (none, 25,25,4)
Conv2D + ReLU	Input: (none, 25, 25, 4)	Conv2D + ReLU	Input: (none, 25, 25, 4)
	Output: (none, 23,23,64)		Output: (none, 23,23,64)
MaxPool	Input: (none, 23, 23, 64)	MaxPool	Input: (none, 23, 23, 64)
	Output: (none, 11,11,64)		Output: (none, 11,11,64)
Conv2D + ReLU	Input: (none, 11, 11, 64)	Conv2D + ReLU	Input: (none, 11, 11, 64)
	Output: (none, 9, 9, 64)		Output: (none, 9, 9, 64)
MaxPool	Input: (none, 9, 9, 64)	MaxPool	Input: (none, 9, 9, 64)
	Output: (none, 4, 4, 64)		Output: (none, 4, 4, 64)
Conv2D + ReLU	Input: (none, 4, 4, 64)	Conv2D + ReLU	Input: (none, 4, 4, 64)
	Output: (none, 2, 2, 32)		Output: (none, 2, 2, 32)
MaxPool	Input: (none, 2, 2, 32)	MaxPool	Input: (none, 2, 2, 32)
	Output: (none, 1, 1, 32)		Output: (none, 1, 1, 32)
Flatten	Input: (none, 1, 1, 32)	Flatten	Input: (none, 1, 1, 32)
	Output: (none, 32)		Output: (none, 32)
Dense + ReLU	Input: (none, 32)	LSTM + ReLU	Input: (none, 32)
	Output: (none, 64)		Output: (none, 1,000)
Dropout	Input: (none, 64)	Dropout	Input: (none, 1,000)
	Output: (none, 64)		Output: (none, 1,000)
Dense	Input: (none, 64)	Dense	Input: (none, 1,000)
	Output: (none, 5)		Output: (none, 5)

Saba, Rehman, Al-Dhelaan, & Al-Rodhaan, 2014b; Saba, Rehman, Altameem, & Uddin, 2014a; Saba, Rehman, & Sulong, 2010). Tahir et al. (2019) conducted a comprehensive study of preprocessing techniques and their effect on feature extraction from medical images. Their explored methods include noise removal, bias correction and removal of unwanted distortion. To remove noise, a Gaussian filter is used by smoothing the image. The contrast enhancement technique of histogram equalization enhances the brightness of an image by normalizing the image intensity distribution whereas the technique of unsharp masking uses the blurred negative image for edge enhancement (Alkawaz, Sulong, Saba, & Rehman, 2016; Fadhil, Alkawaz, Rehman, & Saba, 2016; Waheed, Alkawaz, Rehman, Almazyad, & Saba, 2016). Authors proposed technique is tested to segment and classify related tasks on different medical image sets. Examples from the list of combinations are listed in Table 1. Best performing preprocessing combination of Gaussian Filter, Histogram Equalization and Unsharp Masking is applied on the BRATS2015 data set to come up with better quality images. Additional preprocessing techniques of bias removal, normalization and standardization are applied to data set before proceeding towards segmentation. Bias removal is a technique to remove the bias field, a low-frequency signal which corrupts MRI images due to in-homogeneity in a magnetic field. Bias field distorts the high-frequency signals like edges and changes in intensity field and it is done by using N4ITK algorithm which is an extended form of N3. Next preprocessing technique applied is Normalization, which is the process of changing the range of pixels' intensities of the image. The normalization of each as done using the formula as given in Equation (1).

$$I_{\text{new}} = \frac{(I - \text{Min})(\text{Max}_{\text{new}} - \text{Min}_{\text{new}})}{\text{Max} - \text{Min}} + \text{Min}_{\text{new}} \tag{1}$$

where

I_{new} = new pixel value

I = old pixel value

Min = old minimum value

Max = old maximum value

Min_{new} = new minimum value

Max_{new} = new maximum value

Pixel values of BRATS2015 data set images start from zero and go beyond 255 (the standard range of grey scale image pixel values). Finally, standardization was applied to rescale each image pixel values in the range 0–1 as given in Equation (2).

$$I_{new} = \frac{I - \mu}{\sigma} \quad (2)$$

where

I_{new} = new pixel value

μ = image set mean

σ = image set standard deviation

Data set images prior to and after the application of preprocessing methods are shown in Figure 1.

3.3 | Classification models and their training

One of the challenging tasks in machine learning is to handle class imbalance issue. Due to an unequal number of samples of different classes in training data, the trained model can become biased towards one class leading to model poor performance (Rehman, Abbas, Saba, Mahmood, et al., 2018c; Rehman, Abbas, Saba, Mehmood, et al., 2018b; Rehman, Abbas, Saba, Rahman, et al., 2018a). To address this problem, we worked on three different methods of class balancing as listed below:

- *No balancing:* Training models without any class imbalance handling technique.
- *Sample-based balancing:* Let U is set of all patches, equal number of random samples (E) from each class are selected and these samples are assumed to be representative of its particular class. The selected samples, forming the set of balanced samples of each class, are used to initially train the model and remaining samples (U–E) are used to fine-tune the layers of the trained model.
- *Weight-based balancing:* Relative weights of each tumor class are calculated using a method described in Badrinarayanan, Kendall, and Cipolla (2015). These weights are used during error/loss calculation in the final layer of the neural network. The weights are calculated for each input batch instead of universal weights that are calculated for complete training data set.

Each model is trained separately with each class-imbalance-handling technique as listed above and comparison of obtained results is made to find the best class imbalance handling method before formulating the ensemble of networks.

Classification models: We used three different classification models as described below:

(1) Fully convolution neural network (FCN).

(2) LSTM based convolution neural network (RNN).

(3) Ensemble model based on FCN and LSTM (FNC + RNN).

TABLE 3 DICE similarity values of models trained using no class balancing

S#	Model name	Dice similarity values		
		Complete	Core	Enhancing
1	ConvNet	0.7025	0.6185	0.6578
2	ConvLSTM	0.6895	0.6213	0.5128
3	ConvNet+ ConvLSTM	0.7125	0.6429	0.5418

TABLE 4 DICE similarity values of models trained using sample based balancing

S#	Model name	Dice similarity values		
		Complete	Core	Enhancing
1	ConvNet	0.7824	0.7123	0.6945
2	ConvLSTM	0.8174	0.7081	0.6743
3	ConvNet+ ConvLSTM	0.8329	0.8094	0.7826

CNN model: The convolutional neural network contains the convolutional layers for feature extraction while the fully connected layer is used to find final classification probabilities of each pixel based on patch representing the pixel.

LSTM model: In this model, convolutional layers are used for feature extraction while the final classification of each pixel is performed using LSTM based sequence learning model.

Ensemble model: An ensemble is created using both CNN and LSTM augmented method to select the best prediction of both. Table 2 shows the details of both models.

Each model uses four blocks of layers and each block consists of convolution layers followed by activation and max-pooling layer. To avoid overfitting, dropout layer is used in both models as second last layer in the model. For convolution, we used filters of size 3×3. Max pooling is done to reduce the image size to its half and 0.5 value is used for drop out ratio. For training, a learning rate of 0.1 is used with Adam optimizer (Kingma & Ba, 2014) and categorical cross entropy is used as loss function Equation (3).

$$\mathrm{CCE} = -\left(\frac{1}{N}\right)\sum_{1}^{n}\sum_{j=1}^{n} y_i.\log\left(y_i'\right) \quad (3)$$

Each network is trained for 25 epochs.

Ensemble model: Sequence learning and convolutional models are merged to form an ensemble to study the impact of a joint model for classification. Results obtained through each model are accumulated by averaging final pixel probabilities. Detailed working of this phase in a generalized way is given as follows:

Let there are n models{model_1, model_2, model_3, … , model_n}and each model produces final class probabilities for each of m pixels as (Equation (4))

$$P_1 = \{pc_{11}, pc_{12}, pc_{13}, \ldots, pc_{1m}\},$$
$$P_2 = \{pc_{21}, pc_{22}, pc_{23}, \ldots, pc_{2m}\},$$
$$, \ldots,$$
$$P_n = \{pc_{n1}, pc_{n2}, pc_{n3}, \ldots, pc_{nm}\} \quad (4)$$

TABLE 5 DICE similarity values of model trained using class weighting

S#	Model name	Dice similarity values		
		Complete	Core	Enhancing
1	ConvNet	0.7521	0.6952	0.7145
2	ConvLSTM	0.8114	0.6984	0.6585
3	ConvNet+ ConvLSTM	0.8200	0.7991	0.7741

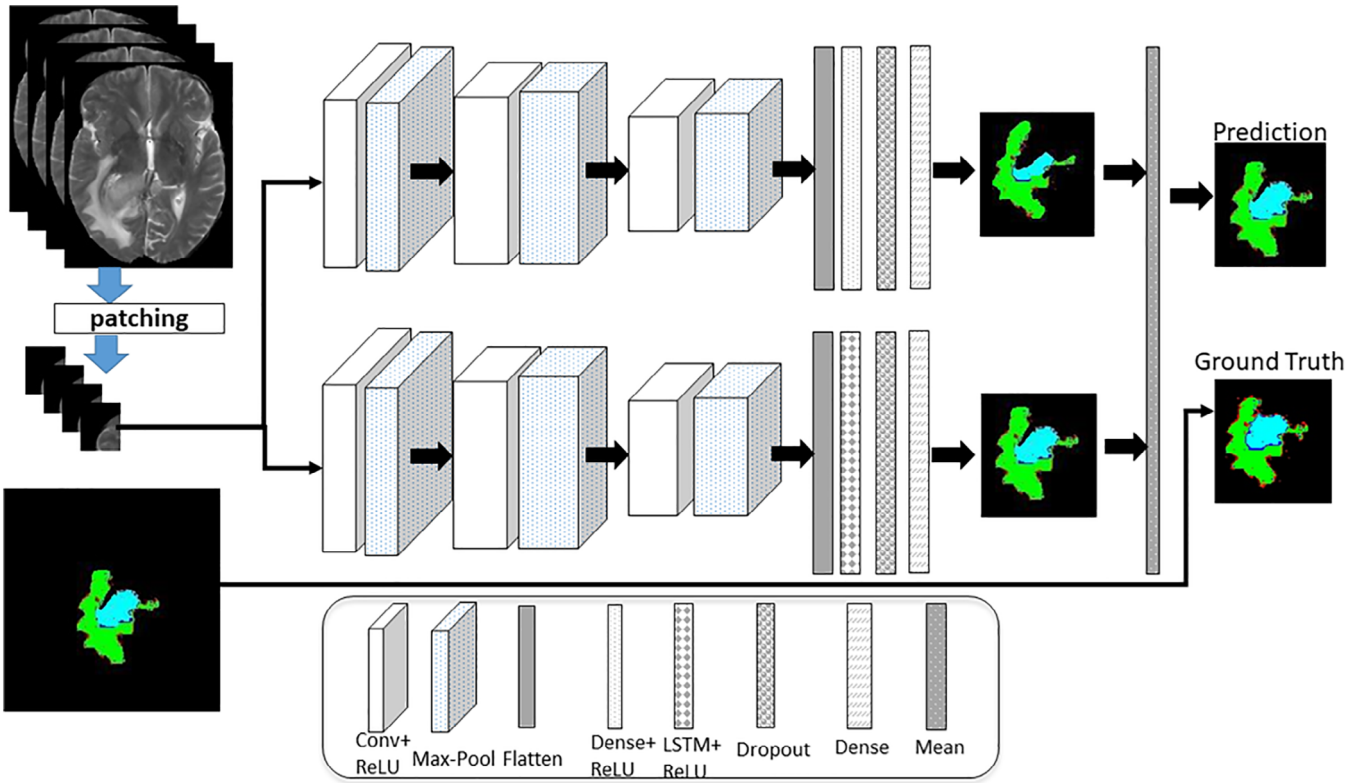

FIGURE 2 Proposed ensemble model [Color figure can be viewed at wileyonlinelibrary.com]

where pc_{nm} represents the probability of pixel-n to lie in class n by model m. The average score of ensemble model can be described by following Equation (5).

$$P_{\text{final}} = \max\left(\begin{array}{c} \dfrac{pc_{11}+pc_{21}+\ldots+pc_{m1}}{m}, \\ \dfrac{pc_{12}+pc_{22}+\ldots+pc_{m2}}{m}, \\ \ldots, \dfrac{pc_{1n}+pc_{2n}+\ldots.+pc_{mn}}{m} \end{array}\right) \tag{5}$$

4 | IMPLEMENTATION AND RESULTS

4.1 | Training

Keras NN library is used for building, training and testing of classification models with TensorFlow as backend. The Adam optimizer (Kingma & Ba, 2014) with categorical cross-entropy as loss function is used to train the model. The formula for categorical cross entropy is given in Equation (6).

$$\text{CCE} = \left(-\frac{1}{N}\right)\left(\sum_{i=0}^{N}\sum_{j=0}^{M} y_j * \log\left(y'_j\right) + (1-y_j) * \log\left(1-y'_j\right)\right) \tag{6}$$

where

N = number of samples

M = number of output nodes

y = labeled output

y' = model prediction

We use 10 million patches from training data set, as described in Section 3.1, to train all three models. In order to avoid excessive and unwanted computation patch filtering is performed where only those patches are used as an input that contains malignant pixels and the amount of such malignant pixels is 100 or more. During training, the network training loss is stabilized after 25 epochs with learning rate fixed at 0.1. Training is performed on a laptop machine installed with Intel Core i5 processor, 4 GB RAM and GeForce gtx 1,050 with 2 GB memory. The training process took 8–10 days to train each model. On average, a trained model took around 90–120 min to segment one sequence of 155 slices on the same machine.

4.2 | Testing and evaluation

Similar to training, patches of size 25×25 are extracted from preprocessed images. The patch around each pixel in the 2D image is created by considering 25×25 pixels around it as neighbor pixels which results in a total number of 57,600 patches from a single 2D image. Boundary pixels are padded with zeros to form a patch of 25×25. The algorithm of testing phase is described as follows:

Algorithm 1 Testing of the proposed methodology

Preprocessing: preprocess as given in the preprocessing section.

$i \leftarrow 0$

for each 2D slice of a sequence

Zero pad 2D slice with zeros

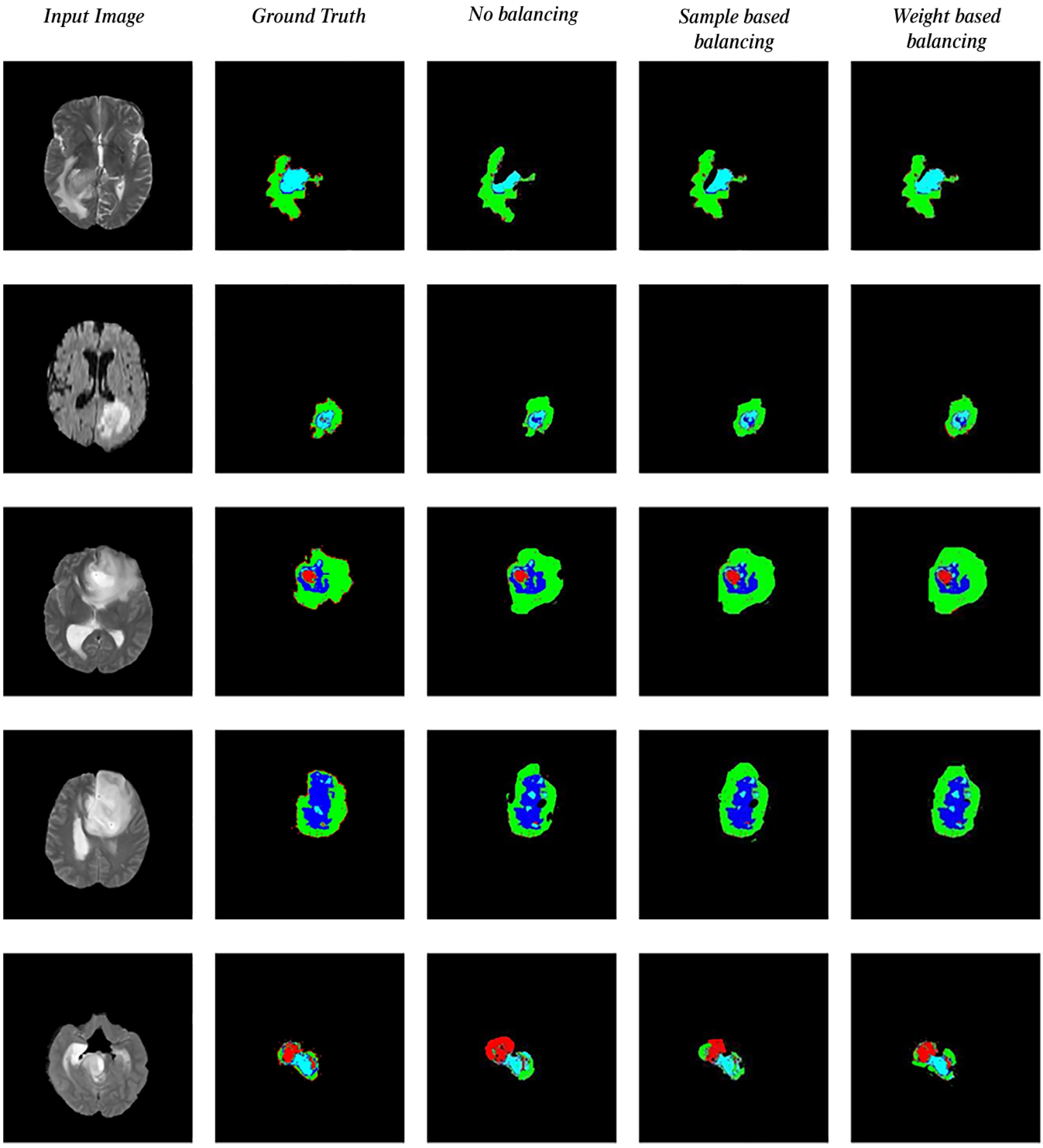

FIGURE 3 CNN network segmentations [Color figure can be viewed at wileyonlinelibrary.com]

Patches← Extract patches of Slice of size 25 × 25
j ← 0
for each path of size 25 × 25
Target Pixel ← Centre of Input patch image
Predict-ConvNet-Class(patch)
Lstm_class ←Predict-Lstm-Class(patch)
Final_class ←Average (Conv_class, Lstm_class)

Evaluation: Predicted classes of models are merged to find segmentation as follows:

Complete: This segmentation is made of pixels of all five classes.

Core: Three types of tumors make this segmentation that is necrosis, enhancing tumor and nonenhancing tumor.

Enhancing: only one type of pixels, that is, enhancing type makes this segmentation.

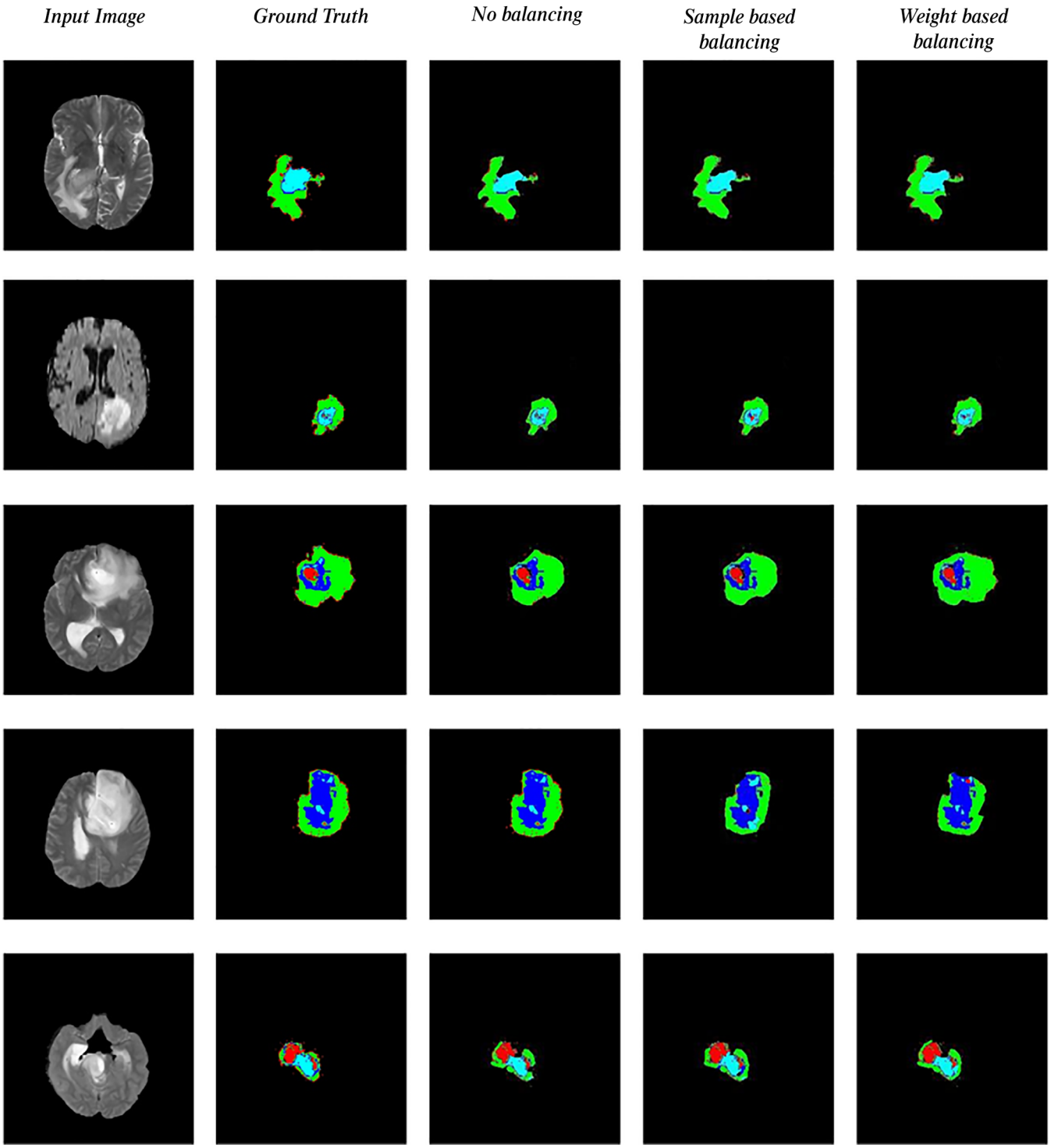

FIGURE 4 LSTM network segmentations [Color figure can be viewed at wileyonlinelibrary.com]

The evaluation of segmentation result is done by using dice similarity coefficient (DSC). Dice similarity measures the overlap area of two images using the formula. If *Seg* is segmentation predicted by the ensemble and is the ground truth then DSC is given by Equation (7):

$$DSC = \frac{(GT \cap SEG)}{(GT \cup SEG)} \tag{7}$$

$\cap$ and $\cup$ are the intersection and union operations respectively.

Tables 3–5 show the dice similarity values of models trained using different class imbalance handling techniques. Figures 2–5 show the segmentation results of convolutional neural network, LSTM based network and ensemble network respectively.

The results presented in Table 3 shows that imbalance class distribution impacts the overall results in negative manners. It is due to the

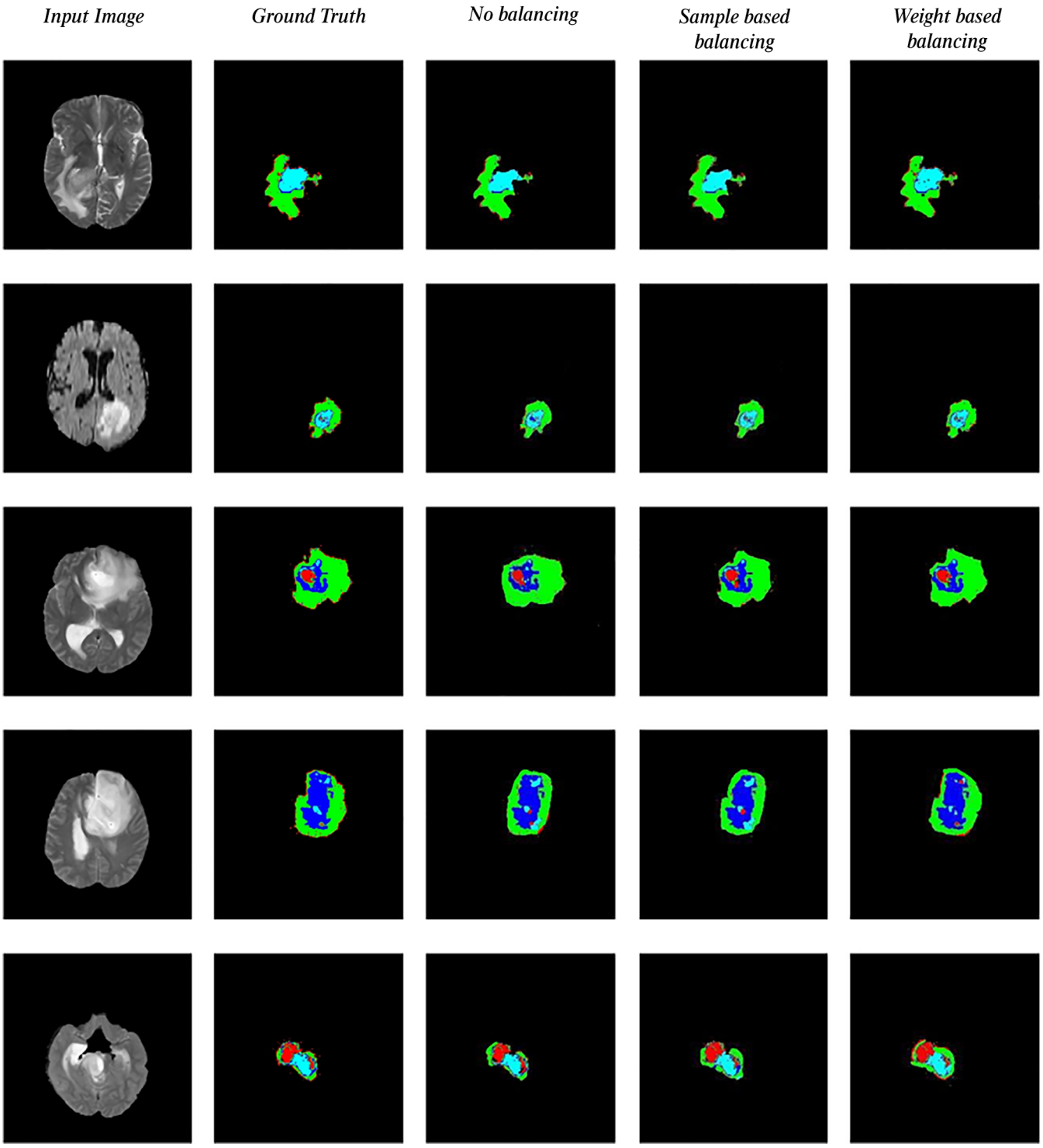

FIGURE 5 Ensemble model segmentations [Color figure can be viewed at wileyonlinelibrary.com]

fact that the majority class dominates the minority classes and results are biased in favor of the majority class. We observe that class balancing trick could improve the results significantly.

The comparison of convolutional neural networks and Convolutional LSTM networks performance is made in this study. The sequence learning models demonstrate competitive performance over convolutional networks. It shows the usability of LSTM based networks in the segmentation task. We can observe that in a given input image the chance of current pixel to belong to the class of its predecessor pixel is higher than that of a different class. This pixel class correlation motivated us to use LSTM based networks for image segmentation task where an LSTM neuron can remember the class of the previous pixel and this observation is assisted to predict the class of new pixel. Finally, both models are ensemble to study the joint impact on brain tumor segmentation.

In this part, we compare the results of proposed models with other states of the art methods published in near past. The

TABLE 6 Comparison of results with other models

Model name	Dice similarity values		
	Complete	Core	Enhancing
Adversarial neural network(Xue et al., 2018)	0.85	0.67	0.63
CNN model(Pereira et al., 2016b)	0.79	0.65	0.75
3D CNN model(Kamnitsas et al., 2017)	**0.95**	0.75	0.72
Deep neural networks(Havaei et al., 2017)	0.79	0.58	0.69
Sequence learning model(Tseng et al., 2017)	0.85	0.68	0.68
Proposed model	0.82	**0.79**	**0.77**

Bold values show main achieved results.

comparison is made with Adversarial convolutional neural network (Xue et al., 2018), CNN (Pereira et al., 2016b), 3D CNN (Kamnitsas et al., 2017), deep neural network (Havaei et al., 2017) and convolutional Sequence Learning model (Tseng et al., 2017). The mentioned adversarial network deploys fully 2D convolutional network as encoder and decoder for segmentation and in 3D CNN three dimensional image is provided to the convolutional network for final segmentation. The CNN and deep neural networks deploy 2D convolution for segmentation. The convolutional sequence learning model deploys a CNN encoder and decoder model but keep an LSTM layer in middle to learn the sequence relations. Our proposed model differs with this model in two aspects (a) it uses CNN as feature extractor and LSTM as the final layer of segmentation for class identification (b) co-relation of image pixels is manipulated at patch level instead of computing for each pixel separately. The result comparison could be seen in Table 6.

Table 6 shows that although proposed model does not perform better in overall segmentation however, next two segmentations, that is, core and enhancing are better to others. Proposed model is fast and robust in a sense it uses few layers as compared to other models which use dozens or even hundreds of layers.

5 | CONCLUSION

This research has presented a light weight neural network based model to segment the brain tumor MRI images using supervised learning method. A number of contributions are achieved such as adaptation of sequence learning models to perform the classification task, the use of ensemble for segmentation task, impact of class balancing on classification and segmentation task and presentation of light weight network architecture for segmentation. The dice similarity score computed for convolutional network is 75% whereas DSC score for LSTM based network is 80%. This exhibits the usefulness of LSTM layers in classification and segmentation work. Combined score of both networks in the form of ensemble is 82.29% which further shows the usability of ensemble models. Reported results confirm that sequence learning based models are equally powerful for segmentation and classification tasks as compared to fully connected and neural network based models. As future work, we intend to explore deeper level of correlation of pixels using modified LSTM networks.

ACKNOWLEDGMENT

This work was supported by Artificial Intelligence and Data Analytics (AIDA) Lab Prince Sultan University Riyadh Saudi Arabia. Authors are thankful for the partial support.

ORCID

Sajid Iqbal https://orcid.org/0000-0003-1760-7653
Tanzila Saba https://orcid.org/0000-0003-3138-3801

REFERENCES

Abbas, N., Saba, T., Mohamad, D., Rehman, A., Almazyad, A. S., & Al-Ghamdi, J. S. (2018a). Machine aided malaria parasitemia detection in Giemsa-stained thin blood smears. *Neural Computing and Applications*, *29*(3), 803–818. https://doi.org/10.1007/s00521-016-2474-6

Abbas, N., Saba, T., Rehman, A., Mehmood, Z., kolivand, H., Uddin, M., & Anjum, A. (2018b). Plasmodium life cycle stage classification based quantification of malaria parasitaemia in thin blood smears. *Microscopy Research and Technique*, *82*, 283–295. https://doi.org/10.1002/jemt.23170

Abbas, A., Saba, T., Rehman, A., Mehmood, Z., Javaid, N., Tahir, M., … Shah, R. (2019). Plasmodium species aware based quantification of malaria, parasitemia in light microscopy thin blood smear. *Microscopy Research and Technique*. https://doi.org/10.1002/jemt.23269

Abbas, N., Mohamad, D., Abdullah, A. H., Saba, T., Al-Rodhaan, M., & Al-Dhelaan, A. (2015). Nuclei segmentation of leukocytes in blood smear digital images. *Pakistan Journal of Pharmaceutical Sciences*, *28*(5), 1801–1806.

Al-Ameen, Z., Sulong, G., Rehman, A., Al-Dhelaan, A., Saba, T., & Al-Rodhaan, M. (2015). An innovative technique for contrast enhancement of computed tomography images using normalized gamma-corrected contrast-limited adaptive histogram equalization. *EURASIP Journal on Advances in Signal Processing*, *32*, 1–12.

Alkawaz, M. H., Sulong, G., Saba, T., & Rehman, A. (2016). Detection of copy-move image forgery based on discrete cosine transform. *Neural Computing and Applications*. https://doi.org/10.1007/s00521-016-2663-3

Aurangzeb, K. I. H., Muhammad Attique, K., Saba, T., Javed, K., & Iqbal, T. (2019). Human behavior analysis based on multi-types features fusion and Von Nauman entropy based features reduction. *Journal of Medical Imaging and Health Informatics*, *9*(4), 662–669.

Badrinarayanan, V., Kendall, A., & Cipolla, R. (2015). Segnet: A deep convolutional encoder–decoder architecture for image segmentation. arXiv preprint arXiv:1511.00561.

Byeon, W., & Breuel, T. M. (2014). Supervised texture segmentation using 2D LSTM networks. *Image Processing (ICIP), 2014 IEEE International Conference on. IEEE*.

Castillo, L. S., et al. (2017). Volumetric multimodality neural network for brain tumor segmentation. *13th International Conference on Medical Information Processing and Analysis*. Vol. 10572. International Society for Optics and Photonics.

Chaudhry, H., Rahim, M. S. M., Saba, T., & Rehman, A. (2018). Crowd region detection in outdoor scenes using color spaces. *International Journal of Modeling, Simulation, and Scientific Computing*, *9*(2), 1–15.

Chen, J., et al. (2016). Combining fully convolutional and recurrent neural networks for 3D biomedical image segmentation. USA. In *Advances in neural information processing systems*.

Ebrahim, A. Y., Kolivand, H., Rehman, A., Rahim, M. S. M., & Saba, T. (2018). Features selection for offline handwritten signature verification: state of the art. *International Journal of Computational Vision and Robotics*, *8*(6), 606–622.

Fahad, H. M., Khan, M. U. G., Saba, T., Rehman, A., & Iqbal, S. (2018). Microscopic abnormality classification of cardiac murmurs using ANFIS and HMM. *Microscopy Research and Technique*, *81*(5), 449–457. https://doi.org/10.1002/jemt.22998

Fadhil, M. S., Alkawaz, M. H., Rehman, A., & Saba, T. (2016). Writers identification based on multiple windows features mining. *3D Research*, *7*(1), 1–6. https://doi.org/10.1007/s13319-016-0087-6

Haji, M. S., Alkawaz, M. H., Rehman, A., & Saba, T. (2019). Content-based image retrieval: a deep look at features prospectus. *International Journal of Computational Vision and Robotics*, *9*(1), 14–38.

Havaei, M., Davy, A., Warde-Farley, D., Biard, A., Courville, A., Bengio, Y., … Larochelle, H. (2017). Brain tumor segmentation with deep neural networks. *Medical Image Analysis*, *35*, 18–31.

Husham, A., Alkawaz, M. H., Saba, T., Rehman, A., & Alghamdi, J. S. (2016). Automated nuclei segmentation of malignant using level sets. *Microscopy Research and Technique*, *79*(10), 993–997. https://doi.org/10.1002/jemt.22733

Iqbal, S., Ghani, M. U., Saba, T., & Rehman, A. (2018). Brain tumor segmentation in multi-spectral MRI using convolutional neural networks (CNN). *Microscopy Research and Technique*, *81*(4), 419–427. https://doi.org/10.1002/jemt.22994

Iqbal, S., Khan, M. U. G., Saba, T., & Rehman, A. (2017). Computer assisted brain tumor type discrimination using magnetic resonance imaging features. *Biomedical Engineering Letters*, *8*(1), 5–28. https://doi.org/10.1007/s13534-017-0050-3

Iftikhar, S., Fatima, K., Rehman, A., Almazyad, A. S., & Saba, T. (2017). An evolution based hybrid approach for heart diseases classification and associated risk factors identification. *Biomedical Research*, *28*(8), 3451–3455.

Jamal, A., Hazim Alkawaz, M., Rehman, A., & Saba, T. (2017). Retinal imaging analysis based on vessel detection. *Microscopy Research and Technique*, *80*(17), 799–811. https://doi.org/10.1002/jemt

Joudaki, S., Mohamad, D., Saba, T., Rehman, A., Al-Rodhaan, M., & Al-Dhelaan, A. (2014). Vision-based sign language classification: a directional review. *IETE Technical Review*, *31*(5), 383–391. https://doi.org/10.1080/02564602.2014.961576

Kamnitsas, K., Ledig, C., Newcombe, V. F. J., Simpson, J. P., Kane, A. D., Menon, D. K., … Glocker, B. (2017). Efficient multi-scale 3D CNN with fully connected CRF for accurate brain lesion segmentation. *Medical Image Analysis*, *36*, 61–78.

Katuka, J. I., Mohamad, D., Saba, T., El-Affendi, M., & Mohamed, A. S. (2014). An analysis of object appearance information and context based classification. *3D Research*, *5*(24). https://doi.org/10.1007/s13319-014-0024-5

Kingma, D. P., & Ba, J.. (2014). Adam: A method for stochastic optimization. arXiv preprint arXiv:1412.6980.

Khan, M. A., Akram, T., Sharif, M., Awais, M., Javed, K., Ali, H., & Saba, T. (2018). CCDF: Automatic system for segmentation and recognition of fruit crops diseases based on correlation coefficient and deep CNN features. *Computers and Electronics in Agriculture*, *155*, 220–236.

Khan, S. A., Nazir, M., Khan, M. A., Saba, T., Javed, K., Rehman, A., … Awais, M. (2019a). Lungs nodule detection framework from computed tomography images using support vector machine. *Microscopy Research and Technique*. https://doi.org/10.1002/jemt.23275

Khan, M. A., Akram, T., Sharif, M., Saba, T., Javed, K., Lali, I. U., … Rehman, A. (2019b). Construction of saliency map and hybrid set of features for efficient segmentation and classification of skin lesion. *Microscopy Research and Technique*. https://doi.org/10.1002/jemt.23220

Khan, M. A., Lali, I. U., Rehman, A., Ishaq, M., Sharif, M., Saba, T., … Akram, T. (2019c). Brain tumor detection and classification: A framework of marker-based watershed algorithm and multilevel priority features selection. *Microscopy Research and Technique*. https://doi.org/10.1002/jemt.23238

Li, Z., Gan, Y., Liang, X., Yu, Y., Cheng, H., & Lin, L. (2016). LSTM-CF: Unifying context modeling and fusion with LSTMS for RGB-D scene labeling. In *European Conference on Computer Vision*. Cham: Springer.

Liang, X., Shen, X., Feng, J., Lin, L., & Yan, S. (2016). Semantic object parsing with graph LSTM. In *European Conference on Computer Vision*. Cham: Springer.

Louis, D. N., Perry, A., Reifenberger, G., von Deimling, A., Figarella-Branger, D., Cavenee, W. K., … Ellison, D. W. (2016). The 2016 World Health Organization classification of tumors of the central nervous system: A summary. *Acta Neuropathologica*, *131*(6), 803–820.

Meethongjan, K., Dzulkifli, M., Rehman, A., Altameem, A., & Saba, T. (2013). An intelligent fused approach for face recognition. *Journal of Intelligent Systems*, *22*(2), 197–212. https://doi.org/10.1515/jisys-2013-0010

Menze, B. H., et al. (2015). The multimodal brain tumor image segmentation benchmark (BRATS). *IEEE Transactions on Medical Imaging*, *34*(10), 1993–2024.

Muhsin, Z. F., Rehman, A., Altameem, A., Saba, A., & Uddin, M. (2014). Improved quadtree image segmentation approach to region information. *The Imaging Science Journal*, *62*(1), 56–62. https://doi.org/10.1179/1743131X13Y.0000000063

Mughal, B., Muhammad, N., Sharif, M., Rehman, A., & Saba, T. (2018). Removal of pectoral muscle based on topographic map and shape-shifting silhouette. *BMC Cancer*, *18*, 778. https://doi.org/10.1186/s12885-018-4638-5

Mughal, B., Muhammad, N., Sharif, M., Saba, T., & Rehman, A. (2017a). Extraction of breast border and removal of pectoral muscle in wavelet domain. *Biomedical Research*, *28*(11), 5041–5043.

Mughal, B., Sharif, M., Muhammad, N., & Saba, T. (2017b). A novel classification scheme to decline the mortality rate among women due to breast tumor. *Microscopy Research and Technique*, *81*, 171–180. https://doi.org/10.1002/jemt.22961

Mundher, M., Muhamad, D., Rehman, A., Saba, T., & Kausar, F. (2014). Digital watermarking for images security using discrete slantlet transform. *Applied Mathematics and Information Sciences*, *8*(6), 2823–2830. https://doi.org/10.12785/amis/080618

Nasir, M., Khan, M. A., Sharif, M., Lali, I. U., Saba, T., & Iqbal, T. (2018). An improved strategy for skin lesion detection and classification using uniform segmentation and feature selection based approach. *Microscopy Research and Technique*, *81*(6), 528–543.

Neamah, K., Mohamad, D., Saba, T., & Rehman, A. (2014). Discriminative features mining for offline handwritten signature verification. *3D Research*, *5*(2). https://doi.org/10.1007/s13319-013-0002-3

Norouzi, A., Rahim, M. S. M., Altameem, A., Saba, T., Rada, A. E., Rehman, A., & Uddin, M. (2014). Medical image segmentation methods, algorithms, and applications. *IETE Technical Review*, *31*(3), 199–213. https://doi.org/10.1080/02564602.2014.906861

Pawar, K., et al. (2017). Residual encoder and convolutional decoder neural network for Glioma segmentation. In *International MICCAI Brainlesion Workshop*. Cham: Springer.

Pereira, S., Pinto, A., Alves, V., & Silva, C. A. (2016a). Deep convolutional neural networks for the segmentation of Gliomas in multi-sequence MRI. In A. Crimi, B. Menze, O. Maier, M. Reyes, & H. Handels (Eds.), *Brainlesion: Glioma, multiple sclerosis, stroke and traumatic brain injuries. BrainLes 2015. Lecture notes in computer science* (Vol. 9556). Cham: Springer.

Pereira, S., et al. (2016b). Brain tumor segmentation using convolutional neural networks in MRI images. *IEEE Transactions on Medical Imaging*, *35*(5), 1240–1251.

Rad, A. E., Rahim, M. S. M., Rehman, A., Altameem, A., & Saba, T. (2013). Evaluation of current dental radiographs segmentation approaches in computer-aided applications. *IETE Technical Review*, *30*(3), 210–222.

Rad, A. E., Rahim, M. S. M., Rehman, A., & Saba, T. (2016). Digital dental X-ray database for caries screening. *3D Research*, *7*(2), 1–5. https://doi.org/10.1007/s13319-016-0096-5

Rahim, M. S. M., Norouzi, A., Rehman, A., & Saba, T. (2017a). 3D bones segmentation based on CT images visualization. *Biomedical Research*, *28*(8), 3641–3644.

Rahim, M. S. M., Rehman, A., Kurniawan, F., & Saba, T. (2017b). Ear biometrics for human classification based on region features mining. *Biomedical Research*, *28*(10), 4660–4664.

Ren, M., & Zemel, R. S. (2017). End-to-end instance segmentation with recurrent attention. *Proceedings of the 2017 IEEE Conference on Computer Vision and Pattern Recognition (CVPR)*, Honolulu, HI.

Rehman, A., Abbas, N., Saba, T., Rahman, S. I. U., Mehmood, Z., & Kolivand, K. (2018a). Classification of acute lymphoblastic leukemia using deep learning. *Microscopy Research & Technique*, *81*(11), 1310–1317. https://doi.org/10.1002/jemt.23139

Rehman, A., Abbas, N., Saba, T., Mehmood, Z., Mahmood, T., & Ahmed, K. T. (2018b). Microscopic malaria parasitemia diagnosis and grading on benchmark datasets. *Microscopic Research and Technique*, *81*(9), 1042–1058. https://doi.org/10.1002/jemt.23071

Rehman, A., Abbas, N., Saba, T., Mahmood, T., & Kolivand, H. (2018c). Rouleaux red blood cells splitting in microscopic thin blood smear images via local maxima, circles drawing, and mapping with original RBCs. *Microscopic Research and Technique*, *81*(7), 737–744. https://doi.org/10.1002/jemt.23030

Saba, T. (2016). Pixel intensity based cumulative features for moving object tracking (MOT) in darkness. *3D Research*, *7*(10), 1–6. https://doi.org/10.1007/s13319-016-0089-4

Saba, T. (2018). Fuzzy ARTMAP approach for arabic writer identification using novel features fusion. *Journal of Computer Science*, *14*(2), 210–220. https://doi.org/10.3844/jcssp.2018.210.220

Saba, T., & Alqahtani, F. A. (2013). Semantic analysis based forms information retrieval and classification. *3D Research*, *4*(3). https://doi.org/10.1007/3DRes.03(2013)4

Saba, T., Almazyad, A. S., & Rehman, A. (2016). Online versus offline Arabic script classification. *Neural Computing and Applications*, *27*(7), 1797–1804. https://doi.org/10.1007/s00521-015-2001-1

Saba, T., Khan, S. U., Islam, N., Abbas, N., Rehman, A., Javaid, N., & Anjum, A. (2019). Cloud-based decision support system for the detection and classification of malignant cells in breast cancer using breast cytology images. *Microscopy Research and Technique*.

Saba, T., Al-Zahrani, S., & Rehman, A. (2012). Expert system for offline clinical guidelines and treatment. *Life Science Journal*, *9*(4), 2639–2658.

Saba, T., Rehman, A., Mehmood, Z., Kolivand, H., Uddin, M., & Anjum, A. (2018a). Plasmodium life cycle stage classification based quantification of malaria parasitaemia in thin blood smears. *Microscopy Research and Technique*. https://doi.org/10.1002/jemt.23170

Saba, T., Rehman, A., Mehmood, Z., Kolivand, H., & Sharif, M. (2018b). Image enhancement and segmentation techniques for detection of knee joint diseases: A survey. *Current Medical Imaging Reviews*, *14*(5), 704–715. https://doi.org/10.2174/1573405613666170912164546

Saba, T., Rehman, A., & Sulong, G. (2010). An intelligent approach to image denoising. *Journal of Theoretical and Applied Information Technology*, *17*(2), 32–36.

Saba, T., Rehman, A., & Sulong, G. (2011a). Cursive script segmentation with neural confidence. *International Journal of Innovative Computing and Information Control (IJICIC)*, *7*(7), 1–10.

Saba, T., Rehman, A., & Sulong, G. (2011b). Improved statistical features for cursive character recognition. *International Journal of Innovative Computing, Information and Control (IJICIC)*, *7*(9), 5211–5224.

Saba, T., Bokhari, S. T. F., Sharif, M., Yasmin, M., & Raza, M. (2018c). Fundus image classification methods for the detection of glaucoma: A review. *Microscopy Research and Technique*, *81*, 1105–1121. https://doi.org/10.1002/jemt.23094

Saba, T. (2017). Halal food identification with neural assisted enhanced RFID antenna. *Biomedical Research*, *28*(18), 7760–7762.

Saba, T., Rehman, A., Altameem, A., & Uddin, M. (2014a). Annotated comparisons of proposed preprocessing techniques for script recognition. *Neural Computing and Applications*, *25*(6), 1337–1347. https://doi.org/10.1007/s00521-014-1618-9

Saba, T., Rehman, A., Al-Dhelaan, A., & Al-Rodhaan, M. (2014b). Evaluation of current documents image denoising techniques: A comparative study. *Applied Artificial Intelligence*, *28*(9), 879–887.

Sadad, T., Munir, A., Saba, T., & Hussain, A. (2018). Fuzzy C-means and region growing based classification of tumor from mammograms using hybrid texture feature. *Journal of Computational Science*, *29*, 34–45.

Schubert, L. K., Westerly, D. C., Tomé, W. A., Mehta, M. P., Soisson, E. T., Mackie, T. R., … Paliwal, B. R. (2009). A comprehensive assessment by tumor site of patient setup using daily MVCT imaging from more than 3,800 helical tomotherapy treatments. *International Journal of Radiation Oncology, Biology, Physics*, *73*(4), 1260–1269.

Sedlar, S. (2017). Brain tumor segmentation using a multi-path CNN based method. In *International MICCAI Brainlesion Workshop*. Cham: Springer.

Shaikh, M., et al. (2017). Brain tumor segmentation using dense fully convolutional neural network. In *International MICCAI Brainlesion Workshop*. Cham: Springer.

Sharif, M. K., Akram, M. A., Javed, T., Saba, M. Y., & Rehman, T. (2017). A framework of human detection and action recognition based on uniform segmentation and combination of Euclidean distance and joint entropy-based features selection. *EURASIP Journal on Image and Video Processing*, *2017*(1), 89.

Sharif, U., Mehmood, Z., Mahmood, T., Javid, M. A., Rehman, A., & Saba, T. (2018). Scene analysis and search using local features and support vector machine for effective content-based image retrieval. *Artificial Intelligence Review*, 1–25.

Shen, H., Zhang, J., & Zheng, W. (2017). Efficient symmetry-driven fully convolutional network for multimodal brain tumor segmentation. *Image Processing (ICIP), 2017 IEEE International Conference on. IEEE*.

Stollenga, M. F., et al. (2015). Parallel multi-dimensional LSTM, with application to fast biomedical volumetric image segmentation. *Advances in Neural Information Processing Systems*, 2998–3006.

Tahir, B., Iqbal, S., Khan, M. U. G., Saba, T., Mehmood, Z., Anjum, A., & Mahmood, T. (2019). Feature enhancement framework for brain tumor segmentation and classification. *Microscopy Research and Technique*. https://doi.org/10.1002/jemt.23224

Tseng, K.-L., et al. (2017). Joint sequence learning and cross-modality convolution for 3D biomedical segmentation. *Computer Vision and Pattern Recognition (CVPR), 2017 IEEE Conference on. IEEE*.

Ullah, H., Saba, T., Islam, N., Abbas, N., Rehman, A., Mehmood, Z., & Anjum, A. (2019). An ensemble classification of exudates in color fundus images using an evolutionary algorithm based optimal features selection. *Microscopy Research and Technique*.

Waheed, S. R., Alkawaz, M. H., Rehman, A., Almazyad, A. S., & Saba, T. (2016). Multifocus watermarking approach based on discrete cosine transform. *Microscopy Research and Technique*, *79*(5), 431–437. https://doi.org/10.1002/jemt.22646

Xue, Y., et al. (2018). Segan: Adversarial network with multi-scale l1 loss for medical image segmentation. *Neuro Informatics*, 1–10.

Yousaf, K., Mehmood, Z., Saba, T., Rehman, A., Munshi, A. M., Alharbey, R., & Rashid, M. (2019). Mobile-health applications for the efficient delivery of health care facility to people with dementia (PwD) and support to their carers: A survey. *BioMed Research International*, *2019*, 1–26.

Yousuf, M., Mehmood, Z., Habib, H. A., Mahmood, T., Saba, T., Rehman, A., & Rashid, M. (2018, Article ID 2134395, 13 pages). A novel technique based on visual words fusion analysis of sparse features for

effective content-based image retrieval. *Mathematical Problems in Engineering*, *2018*. https://doi.org/10.1155/2018/2134395

Younus, Z. S., Mohamad, D., Saba, T., Alkawaz, M. H., Rehman, A., Al-Rodhaan, M., & Al-Dhelaan, A. (2015). Content-based image retrieval using PSO and k-means clustering algorithm. *Arabian Journal of Geosciences*, *8*(8), 6211–6224. https://doi.org/10.1007/s12517-014-1584-7

How to cite this article: Iqbal S, Ghani Khan MU, Saba T, et al. Deep learning model integrating features and novel classifiers fusion for brain tumor segmentation. *Microsc Res Tech*. 2019; 82:1302–1315. https://doi.org/10.1002/jemt.23281